

Axial Compression Of Tubular Metallic Shells having combined tube-frusta geometry

P. K. Gupta

(Civil Engineering Dept., Indian Institute of Technology Roorkee, Roorkee (UA) 247667, INDIA)

(email: pkgupfce@iitr.ernet.in)

Abstract

The present paper deals with the experimental and computational study of collapse of the metallic shells having combined tube-frusta geometry subjected to axial compression between two parallel plates. Shells are having top one third lengths as tube and remaining bottom two third length as frusta. Shells were tested to identify their modes of collapse and associated energy absorption capacity. An axisymmetric Finite Element computational model of collapse process is presented and analysed, using a non-linear FE code FORGE2 [17]. Six noded triangular elements were used to discretize the domain. The material of the shells was idealized as rigid visco-plastic. Experimental and computed results of the deformed shapes and their corresponding load-compression and energy-compression curves were compared to validate the computational model. On the basis of the obtained results development of the axisymmetric mode of collapse has been presented, analysed and discussed.

Keywords: axial compression, crashworthiness, metallic shells, energy absorption, FORGE2

1. INTRODUCTION

Thin walled structural shell elements such as cylindrical shells, conical shells, and domes are commonly used as energy absorbing elements in crashworthiness applications. Study of their collapse behaviour has received considerable attention of the researchers in the last four decades. Experimental, analytical and computational studies on these structural elements have been carried out under both quasi-static and dynamic loadings in axial and lateral directions [1-16]. Among the different energy absorbing elements the thin walled conical shells commonly known as frusta are employed over a broad range of applications, especially in the applications of aerospace and armaments as the nose cones of missiles and aircraft.

Johnson and Reid [1] examined and there after reviewed the modes of collapse of and associated load–displacement variations for different thin-walled shells. Postlethwaite and Mills [2] performed the axial crushing tests on conical shells of semi-apical angles of 5–20 degree and studied their energy absorption capacity. Mamalis and Johnson [3] tested aluminum frustas under quasi-static axial compression between two parallel platens to study their crumbling. In experiments they identified two modes of collapse namely concertina and diamond modes and also proposed empirical relationships for both these modes of deformation. Mamalis et al. [4] extended their experimental study to include the effect of strain rate and found that the deformation modes of frusta could be classified as (a) concertina, (b) concertina-diamond, and (c) diamond. Mamalis and associates [5] modified and produced a refined model of Postlethwaite and Mills [2] and obtained a better prediction for the mean crushing load. In another paper, Mamalis and his team [6] modeled the progressive extensible collapse of frusta and presented a theoretical model that shows the changes in peaks and troughs of the experimental load-displacement curves. Their theoretical predictions were fairly comparable with their experimental counterparts.

Others researchers Alghamdi [7], Aljawi and Alghamdi [8], Aljawi and Alghamdi [9], Alghamdi et al. [10,11], El-Sobky et al. [12], and Gupta and Venkatesh [13] have also reported experimental studies on the performance of compressed frusta subjected to quasi-static and dynamic axial loadings. Gupta and Gupta [14-16] also studied the collapse process of metallic shells subjected to axial compression between two flat platens with experiments and FE modeling.

From the previous research results it can be concluded that on the basis of experimental investigations different analytical models have been proposed by different researchers [3-6, and 12]. But the complexity of deformation process often limits the general use of closed-form analytical solutions. Therefore, it is essential to use numerical methods to solve this class of problems in the present time, when computational facilities are enhancing day by day.

The paper presents an experimental and computational analysis of the deformation behaviour of the metallic thin walled shells having combined tube-frusta geometry subjected to axial compression between two parallel plates. Shells are having top one third lengths as tube and remaining bottom two third length as frusta. Shells were tested to identify their modes of collapse and to study the associated energy absorption capacity. Wall thickness of shell was varied. A Finite Element computational model of development of the axisymmetric mode of collapse is presented and analysed, using a non-linear finite element code FORGE2. Experimental and computed results of the deformed shapes and their corresponding load-compression and energy-compression curves were presented and compared to validate the computational model. On the basis of the obtained results development of the axisymmetric mode of collapse has been presented, analysed and discussed.

2. EXPERIMENTS

Aluminium sheets of thicknesses varying between 1 and 5 mm were commercially obtained, and the geometry of the shells required for the present experimental work were made from these sheets by the process of spinning. All the shells were annealed by soaking them at 3000 C in the furnace for 1 hour, and allowing them to cool in the furnace for 24 hours. A universal testing machine Instron of 250 T capacity was employed for experimentation. Specimens were centrally positioned on the bottom platen of the machine with tube diameter touching the top platen of the machine. The upper platen was moved at a constant downward velocity of 10 mm/min. The compression process was continued till the top diameter of tube and folded portion of the shell came in contact with top

platen. The load-compression curves were recorded with the automatic recorder of the machine. The deformed shapes of the specimens at different stages of the compression process were recorded. It was found that in the beginning of the collapse process of all the shells an axisymmetric concertina ring develops at the junction of tube and cone towards the inner side of the cone. There after the tube portion of the shell moves into the remaining portion of the shell with continuous deformation of cone. This process gets continued till tube diameter top end and the concertina fold and deformed shell comes into the contact of the upper platen of the machine. Fig. 1 depicts the photographs of the development of the mode of collapse. It is very clear that the mode of collapse remains axisymmetric throughout its development process. The corresponding experimental load-compression and calculated energy-compression curves for these specimens are presented in Figs. 2(a) and 2(b) respectively. Energy-compression variations are obtained by integrating the load-compression curves.

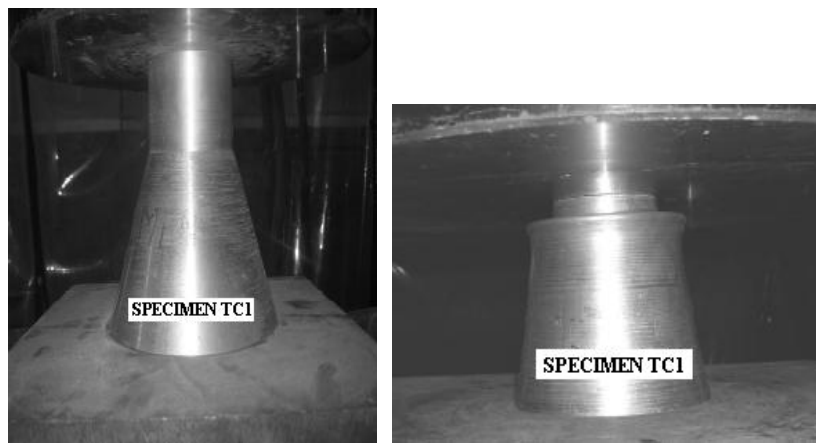


Fig. 1 Typical views of the undeformed and deformed shells.

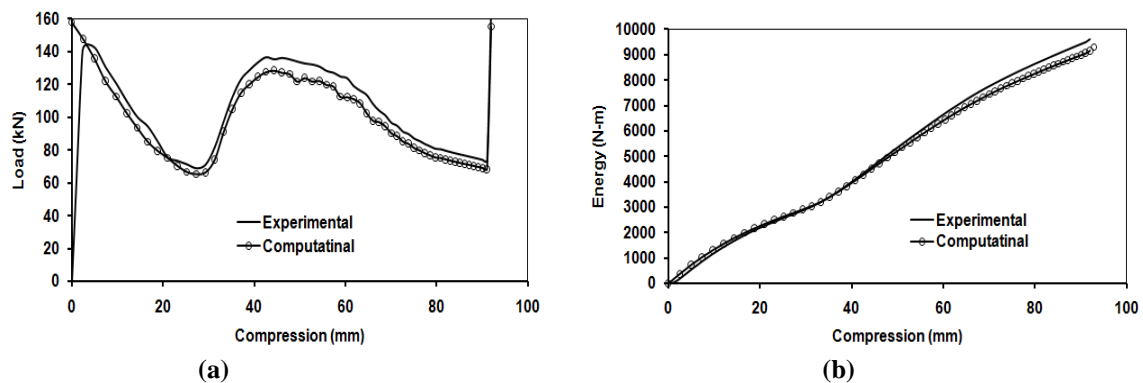


Fig. 2 Comparison of typical (a) load-compression and (b) energy-compression curves for shells.

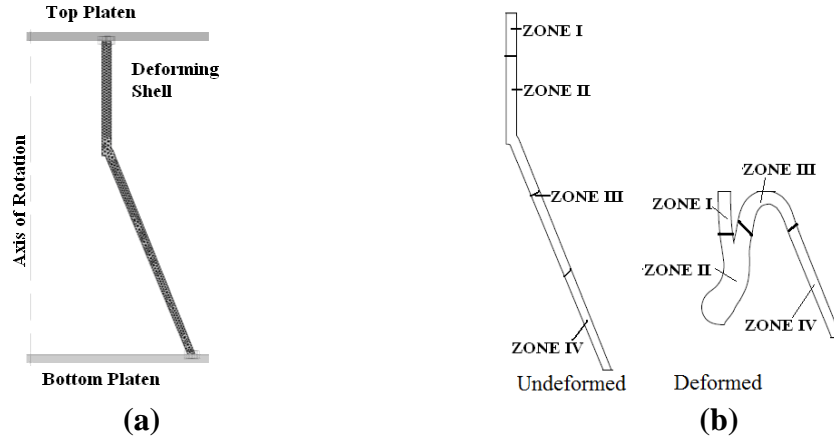


Fig. 3(a). Computational model for axisymmetric deformation, (b) Demarcation of zones in undeformed and a typically deformed shell

3. Computational study

3.1 Governing equations

Finite element formulations for non-linear problems of plasticity are classified into solid formulations and flow formulations. In the flow formulation which is employed here, the elastic components of strain are neglected as small compared to their plastic counterparts. An updated Lagrangian reference system is employed wherein the velocities are considered as the basic unknowns and the incompressibility condition is incorporated using a penalty function. The overall deformation is analysed in terms of a large number of deformation steps. Linearised relationship between the stress and strain rate is assumed to exist during each step and a quasi-steady state is assumed for each incremental solution. The computational procedure is linked to a re-zoning procedure.

Each deformation step is treated as a boundary value problem. At the beginning of a given step, the problem domain Ω (i. e. the volume occupied by the deforming tube), the state of inhomogeneity and the values of material parameters are supposed to be given or determined already. The velocity vector \tilde{v} is prescribed on a part of surface S_v together with traction on the remainder of surface S_f . Solution to the incremental problem at any given time provides the velocity and stress distributions that satisfy the governing equations in the body as well as boundary conditions on the surface. The material is assumed as homogeneous, isotropic, incompressible and rigid visco-plastic. The constitutive relation for such a material is given by the Norton-Hoff law as follows

$$\tilde{S}_{ij} = 2K \left(\sqrt{3} \dot{\tilde{\epsilon}} \right)^{m-1} \tilde{\epsilon}_{ij} \tag{1}$$

$$\text{where } \dot{\tilde{\epsilon}} = \left(\frac{2}{3} \tilde{\epsilon}_{ij} \cdot \dot{\tilde{\epsilon}}_{ij} \right)^{1/2}, \quad \tilde{\epsilon}_{ij} = \frac{1}{2} (v_{i,j} + v_{j,i})$$

where \tilde{S}_{ij} , $\tilde{\epsilon}_{ij}$, K and m represents the components of the deviatoric stress tensor, strain rate tensor, material consistency and strain rate sensitivity index respectively. The v_i is the component of velocity in the direction "i" at any point of the problem domain. The incompressibility condition is written as below

$$\text{div } \tilde{v} = 0 \quad \text{over the problem domain } \Omega \quad (2)$$

where \tilde{v} is the velocity vector at any point of the domain.

The material consistency K depends upon the thermo-mechanical condition of the material. For most metals, the behaviour of K can be approximated by means of the following multiplicative law;

$$K = K_0 (1 + a\bar{\epsilon}) e^{\beta/T} \quad (3)$$

where K_0 is a constant, a is the strain hardening parameter, β is the temperature sensitivity term and T is the absolute temperature. The values of the parameters K_0 , a , β and m can be found by conducting uniaxial tensile tests at different strain rates and temperatures. By suitable choice of these parameters, equations (1) and (3) can approximate the mechanical behaviour of most of the metals at different temperatures and strain rate ranges. Using above equations the constitutive equation for uniaxial case gets the form as follows

$$\bar{\sigma} = K_{ot} (1 + a\bar{\epsilon}) \dot{\bar{\epsilon}}^m \quad (4)$$

where $\bar{\sigma}$ is the equivalent stress for uniaxial case and $K_{ot} = K_0 (\sqrt{3})^{m+1} e^{\beta/T}$

The friction between the shell and the platens is modeled with a viscoplastic law

$$\tau_f = -\alpha K_o (1 + a\bar{\epsilon}) \dot{\bar{\epsilon}}^m \tilde{v}_f \left\| \tilde{v}_f \right\|^{p-1} \quad (5)$$

where $\|\cdot\|$ indicates the norm of a vector, \tilde{v}_f is the sliding velocity between tube and platen, α is the friction factor and p is a material parameter whose value is often taken equal to m . The remeshing of six noded isoparametric triangular elements is achieved through a DeLaunary-Voronoi type algorithm. Values of $\bar{\epsilon}$ at the nodes of the newly created mesh are found by interpolation of the corresponding values at the nodes of the older, distorted mesh.

3.2 COMPUTATIONAL MODEL AND ITS FEATURES

In the finite element model of the compression process the top platen was modeled to move on its axis with a downward velocity of 10 mm/minute while the bottom platen as stationary. The contact between the platen and shell surfaces has been assumed as sliding unilateral [17]. Friction factor α at the platen shell interface is assumed to be given [17]. Since the original and experimentally deformed shells were axisymmetric so an axisymmetric Finite Element model of the compression process is proposed and presented. Fig. 3(a) shows the computational model used for the present investigation. Six noded isoparametric triangular elements have been used to discretize the tube domain. The temperature is kept constant and equal to room temperature 310o K. Compression process of each tube specimen was simulated using FORGE2 code and analyzed. The total deformation of the specimen was carried out into small steps called as increments. The value of the

incremental strain in each increment was taken equal to 2% of the current tube height. Number of elements used for discretization of the problem domain were varied between 900 to 1030. Number of remeshings required to finish the compression of different specimens were between forty five to fifty three. The computer memory required to store the results of these simulations varied from 18 to 20 MB.

The following constitutive relation models mechanical behaviour of the tube material

$$\bar{\sigma} = K_{ot} (1 + a\bar{\epsilon})^{\frac{1}{m}}$$

where, $K_{ot} = K_o (\sqrt{3})^{m+1} e^{\beta/T}$, and $\bar{\sigma}$ is the effective stress, K_o is a constant, a is the strain hardening parameter, m is strain rate sensitivity index, β is the temperature sensitivity term and T is the absolute temperature. If the compression process is performed at a more or less constant temperature then the value of $e^{\beta/T}$ remains same at all points of the deforming body. To determine the above material parameters namely K_o , a and m uniaxial tensile tests were conducted at three different strain rates. Special tensile test specimens were prepared by cutting the same shells in their axial direction as were used for carrying out the compression tests. Load-deformation curves were recorded. The true stress versus true strain curves were calculated from the recorded load-deformation curves to calculate the material parameters.

To verify the proposed Finite Element model typical experimental and computed load-compression and energy-compression curves as well as deformed shapes were compared. Fig. 4 shows typical computed deformed profiles at various stages of compression of shell specimen. Figs. 2(a) and (b) presents the comparison of typical experimental and computed load-compression and energy-compression curves. Comparison of experimental and computed deformed profiles at the end of the compression process is presented in Fig. 5. After seeing the Fig. 2 one can say that the computed load-compression and energy-compression variations have good agreement with the experimental ones. The computed and true deformed shapes are also match quite well (see Fig. 5).

4. DISCUSSION ON TYPICAL COMPUTATIONAL RESULTS

To discuss the compression process four zones of interest have also been demarcated within the shell cross-section. These can be described as,

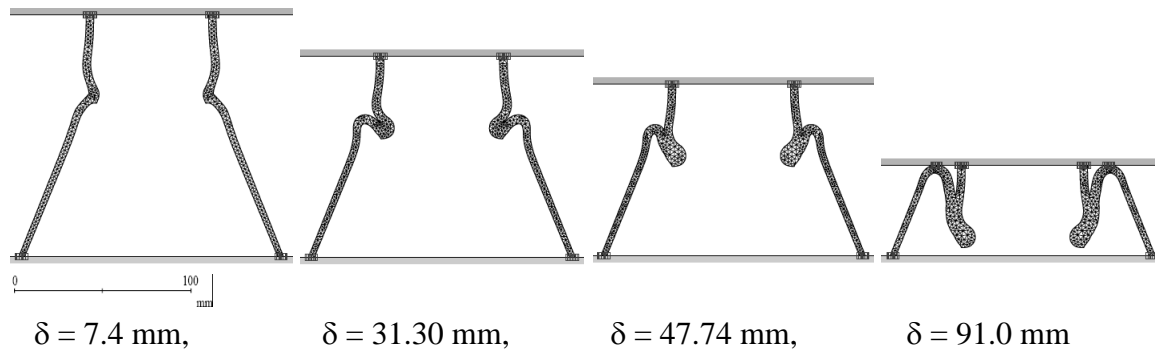


Fig. 4 Typical computed deformed profiles at different values of compression (δ).

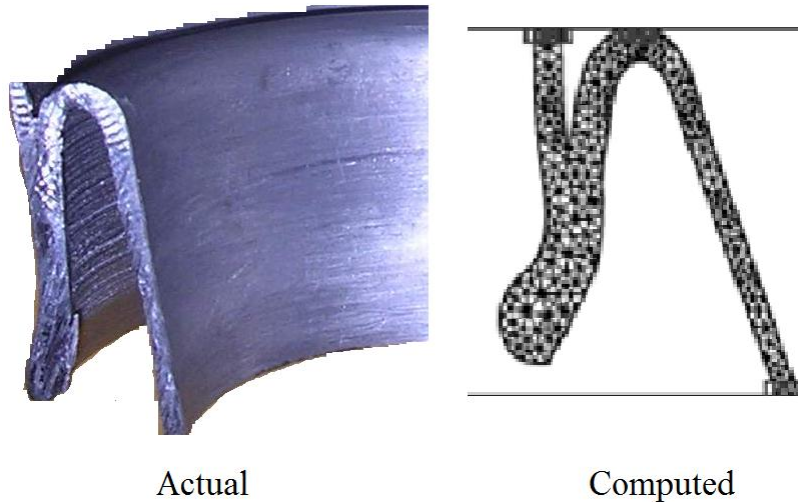


Fig. 5 Comparison of deformed shapes of specimen F5 after compression.

Zone I and IV: Region of the shell adjoining to the top and bottom platens respectively where deformation does not occur.

Zone II: Region of the shell locked between zone I and zone III. During the compression process its area continuously increases.

Zone III: Region of the shell adjoining to the zone II and originated from zone IV

The proposed simulation model was used to obtain detailed computational results of compression of each specimen, however computational results of a typical specimen are presented below. Input data for this typical case is:

$K_0 = 109.3$ MPa, $m = p = 0.0147$, $a = 0.125$, friction factor at top interface (α_{Top}) = 0.45, friction factor at bottom interface (α_{bottom}) = 0.45. The problem domain was discretized into 975 elements. Strain increment in each step of compression was 2%. The total displacement of 91 mm of top platen was completed in 117 steps (increments).

5. DEVELOPMENT OF AXISYMMETRIC MODE OF COLLAPSE

To understand the pattern of deformation occurring during axial compression of shell and development of axisymmetric mode of collapse, the compression process is divided into two stages, referred to as the initial and final.

Initially the shell is having contacts over its whole periphery with the top and bottom platens on both the ends. Therefore, in the beginning of the compression process uniform compression of the shell occurs and the load in the load-compression curve reaches to its peak value. Very soon the local buckling triggered at the junction of tube and cone of the shell and concertina folding begins at that location on the inner side of shell. This is designated as first stage of compression. This stage of

compression is characterized by localized deformation in a region which is identified as region II (marked in Fig. 3(b)). The so-called concertina fold forms there. With increase of compression, the folding progresses and the tube bends more and more. The folding continues at decreasing load because the rate of increase of resistive moment due to strain hardening in region II is less as compared to the increase in the eccentricity (distance between the point of action of load point and the concertina fold in region II). With progress of compression the load continues to decrease but at a lower rate. This is because per unit of compression, the influence of eccentricity increase tends to progressively decrease relative to that of the increase of resistive moment at the concertina fold. The upper arm of the fold remains inclined with the horizontal and in this condition the contact occurs between two outer boundaries of the shell. This is the end of formation of concertina fold. After this stage with further compression the load starts increasing once again and reaches to the second peak value. This may be ascribed to end of the localized bending around the concertina fold and further deformation is mainly confined in this region (concertina fold location) only. During this stage the portion of shell around the concertina fold rotates in such a way that the folded portion gets a particular angle. After this rotation, concertina fold moves radially inward. After this stage with progress of compression, site of dominant deformation expands to the new virgin shell called as zone III and originated from zone IV. As this happens, zone II starts expanding and zone I and zone IV starts reducing. This marks the beginning of the second stage of compression, and spread of the plastic hinge. However the required load is lower as compared to that in initial stage. The plastic hinge continuously moves radially inward with leaving a plastified region (zone II) behind it. At this juncture to expand the plastic region in the virgin shell from zone IV and of larger periphery load required is of lower value due to the increase in lever arm by movement of some portion of tube of zone I inner side. Therefore, the magnitude of compression load decreases in the remaining compression process and development of axisymmetric mode proceeds further.

6. CONCLUSIONS

An experimental and computational study of quasi-static axial compression of metallic thin walled shells having combined tube-frusta geometry between two parallel plates is presented. Shells are having top one third lengths as tube and remaining bottom two third length as frusta. It was found that all these shells were deformed in axisymmetric mode of collapse. A Finite Element computational model of the development of the axisymmetric mode of collapse is also presented. Experimental and computed results of the deformed shapes and their corresponding load-compression and energy-compression curves are compared and found in good agreement. On the basis of the study the mechanics of the mode of collapse has been studied and discussed.

The mode of collapse forms by the development of one concertina fold followed by the plastic zone designated here as zone II. The concertina fold develops fully while plastic zone develops continuously till the end of compression process. During the development of mode of collapse some portions of the shell move radially inward and some radially outward.

Acknowledgements

Author is thankful to Prof. N.K. Gupta and Prof. G.S. Sekhon, Applied Mechanics Department, Indian Institute of Technology, Delhi, India for providing area of research and support. Author is also thankful to Mr. RR Sahu for helping in experiments.

REFERENCES

- [1] Johnson W and Reid SR. (1978) “Metallic energy dissipating systems.” *Appl Mech Rev*; 31:277–88.
- [2] Postlethwaite HE and Mills B. (1970) “Use of collapseible structural elements as impact isolators with special reference to automotive applications.” *J Strain Anal*; 5: 58–73.
- [3] Mamalis AG and Johnson W. (1983) “The quasi-static crumpling of thin-walled circular cylinders and frusta under axial compression.” *Int J Mech Sci*; 25: 713–32.
- [4] Mamalis AG, Johnson W and Vigilant GL. (1984) “The crumbling of steel thin-walled tubes and frusta under axial compression at elevated strain-rate: some experimental results.” *Int J Mech Sci*;26:537–47.
- [5] Mamalis AG, Manolakos DE, Saigal S, Viegelaahn G and Johnson W. (1986) “Extensible plastic collapse of thin-wall frusta as energy absorbers.” *Int J Mech Sci*; 28: 219–29.
- [6] Mamalis AG, Manolakos DE, Viegelaahn GL and Johnson W. (1988) “The modeling of the progressive extensible plastic collapse of thin-wall shells.” *Int J Mech Sci*; 30: 249–61.
- [7] Alghamdi AAA. (1991) “Design of simple collapsible energy absorber.” MSc thesis. College of engineering, King Abdulaziz University, Jeddah, Saudi Arabia.
- [8] Aljawi AAN, Alghamdi AAA.(1999) “Investigation of axially compressed frusta as impact energy absorbers.” In: Gaul L, Brebbia AA, editors. *Computational methods in contact mechanics IV*. Southampton: WIT Press; p. 431–43.
- [9] Aljawi AAN, Alghamdi AAA. (2000) “Inversion of frusta as impact energy absorbers.” In: Hassan MF, Megahed SM, editors. *Current advances in mechanical design and production VII*. New York: Pergamon Press; p. 511–9.
- [10] Alghamdi AAA, Aljawi AAN, Abu-Mansour TMN, Mazi RAA. (2000) “Axial crushing of frusta between two parallel plates.” In: Zhao XL, Grzebieta RH, editors. *Structural failure and plasticity*. New York: Pergamon Press; p. 545–50.
- [11] Alghamdi AAA, Aljawi AAN, Abu-Mansour TMN. (2002) “Modes of axial collapse of unconstrained capped frusta.” *Int J Mech Sci*; 44: 1145–61.

- [12] El-Sobky H, Singace AA, Petsios M. (2001) "Mode of collapse and energy absorption characteristics of constrained frusta under axial impact loading." *Int J Mech Sci*; 43: 743–57.
- [13] Gupta N. K. and Venkatesh (2007) "Experimental and numerical studies of impact axial compression of thin-walled conical shells" *International Journal of Impact Engineering*.
- [14] Gupta P. K. and Gupta N. K. (2006) "Computational and experimental studies of crushing of metallic hemispherical shells" *Archive of Applied Mechanics* 76: 511–524
- [15] Gupta P. K. and Gupta N. K. (2006) "An experimental and computational study of crushing of metallic hemispherical shells between two rigid flat platens" *Journal of Strain Analysis for Engg. Design* Vol. 41, No. 6, pp 453-466.
- [16] Gupta P.K. (2008) "A study on mode of collapse of varying wall thickness metallic frusta subjected to axial compression" *Thin Wall Struct*; 36: 169–79.
- [17] FORGE2. (1996) Finite element analysis code for metal forming problems *version 2.5*, cemef, sofia Antipolis, France 1996.